Determination of the dielectric biaxiality in a chiral smectic-C phase

F. Gouda
Physics Department, Chalmers University of Technology, S-41296 Göteborg, Sweden

W. Kuczynski
Institute of Molecular Physics, Polish Academy of Sciences, Smoluchowskiego 17/19, 60-179 Poznan, Poland

S. T. Lagerwall, M. Matuszczyk, T. Matuszczyk, and K. Skarp
Physics Department, Chalmers University of Technology, S-41296 Göteborg, Sweden
(Received 12 August 1991; revised manuscript received 9 December 1991)

A method is presented allowing the determination of the three principal values $(\varepsilon_1,\varepsilon_2,\varepsilon_3)$ of the dielectric tensor for a chiral smectic-C liquid crystal in the case that the material has an uncompensated helix. Hence it is applicable for essentially all single substances and therefore suitable for developing correlations between molecular structure and dielectric properties of the smectic-C^* materials. The method requires two samples and uses three different measurement geometries. The first sample has the smectic layers parallel to glass plates and is also used for the determination of the tilt angle θ needed in the evaluation of $(\varepsilon_1,\varepsilon_2,\varepsilon_3)$. The two other measurements are made on a sample with the smectic layers essentially perpendicular to the glass plates, allowing chevron or uniformly tilted layer structure in the sample. One measurement is taken in the presence of the helix and another in the nonhelical (unwound) state obtained by applying a bias field. Measurements have been performed on one ester compound exhibiting A^* and C^* phases. The dielectric tensor components have been calculated and are presented as functions of temperature and frequency.

PACS number(s): 61.30.Gd

I. INTRODUCTION

The orthogonal smectic-A phase is uniaxially dielectric, similar to a nematic phase. The dielectric permittivity tensor has two nonzero components that can be measured in a direction parallel ($\varepsilon_\parallel$) and perpendicular ($\varepsilon_\perp$) to the director $\mathbf{n}$. The dielectric anisotropy $\Delta\varepsilon$ is defined as $\varepsilon_\parallel-\varepsilon_\perp$. Tilted smectic phases, e.g., the nonchiral smectic-C or the chiral smectic (C^*) phase, are biaxial dielectrics. The usual definition of dielectric anisotropy does not make sense in the case of tilted smectic phases because of the two nondegenerate components corresponding to $\varepsilon_\perp$. Some authors [1,2] have defined the dielectric anisotropy as the difference between dielectric permittivity measured in a direction parallel and perpendicular to the helix axis, which, however, makes it an operational property difficult to relate to molecular structure.

In the case of tilted smectic phases, it is clear that in order to apply a definition of $\Delta\varepsilon$ that holds also in the orthogonal phases we have to choose the biaxial frame of reference in a suitable way. For the uniaxial nematic and smectic-A phases it is customary [3] to write simple anisotropic properties like dielectric permittivity ε_{ij} or magnetic susceptibility χ_{ij} in the form

$$\varepsilon_{ij}=\begin{pmatrix}\varepsilon_\perp & 0 & 0\\ 0 & \varepsilon_\perp & 0\\ 0 & 0 & \varepsilon_\parallel\end{pmatrix},$$

thus choosing the 3 (or z) axis along the molecular direction. If we look at the transition $A\leftrightarrow C$, according to Fig. 1, we see that $\varepsilon_\parallel$ for the A phase corresponds to ε_3 in the C phase and we can choose ε_1 perpendicular to ε_3 in the direction of the tilt θ, i.e., tilting out of the smectic layer plane by the same angle θ, which gives ε_2 along the direction of the C_2 symmetry axis characteristic of the C phase (which is also the direction of the spontaneous polarization P_S in the case of the smectic-C^* phase). Then the biaxiality can be written as

$$\delta\varepsilon=\varepsilon_2-\varepsilon_1\ ,$$

while for the anisotropy the difference between ε_3 and any of ε_1 or ε_2 could be taken as a measure. We have followed the convention introduced by Jones, Raynes, and Towler [4] and thus write

$$\Delta\varepsilon=\varepsilon_3-\varepsilon_1\ .$$

The three components of the dielectric permittivity tensor have been determined in the chiral smectic-C phase for the first time by Hoffmann *et al.* [5]. Their measurements have been performed at 1 MHz and thus did not include the important low-frequency regime. In their work, the smectic layers of the C^* phase in the planar orientation were assumed to be perpendicular to the glass plates (upright bookshelf geometry). As we know today, this assumption is rarely valid [6].

Recently it has been reported [7] that an ac stabilization effect was observed for compounds with positive

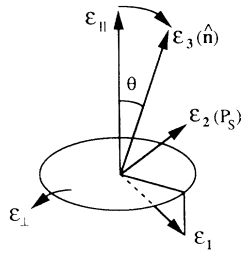

FIG. 1. Orientation of the principal axes of permittivities in uniaxial and biaxial phases. In uniaxial systems, the ε tensor is described by one axis $\varepsilon_{\parallel}$ parallel to the director $\mathbf{n}$ and a degenerate axis $\varepsilon_\perp$ perpendicular to the director lying in any direction in the plane perpendicular to the director. In biaxial systems, the ε tensor is described by three principal axes ε_1, ε_2, and ε_3. At the transition from uniaxial to biaxial, $\varepsilon_{\parallel} \leftrightarrow \varepsilon_3$, $\varepsilon_\perp$ becomes nondegenerate and splits into two components: ε_2 parallel to $\varepsilon_{\parallel} \times \varepsilon_3$, and ε_1, which is perpendicular to the plane containing ε_3 and ε_2.

dielectric anisotropy as defined in Refs. [1] and [2]. As pointed out by Jones and co-workers [4,8], the observed ac field effect on the extinction angle in ferroelectric liquid crystal (FLC) devices cannot be interpreted on the basis of dielectric uniaxiality. These results have direct consequences on the electro-optic properties of FLC devices, and motivate further studies of the dielectric biaxiality. In this paper, we have extended the approach of Ref. [5] and reshaped it to a more closed form. In particular we also discuss the consequences of inclined smectic layers in the C^* phase. Based on three measuring geometries, the calculations allow determination of the three components of the dielectric tensor. The temperature dependences of the dielectric biaxiality and the dielectric anisotropy have been determined at low and high frequencies and their critical exponents are calculated.

II. EXPERIMENT

The dielectric biaxiality in the C^* phase has been determined for the substance

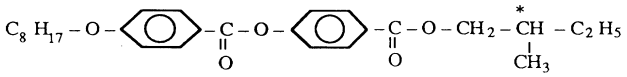

with the transition temperatures

$$\text{crystalline} \xleftarrow[20\,^\circ\text{C}]{} \text{smectic } C^* \xleftarrow[30.2\,^\circ\text{C}]{} \text{smectic } A^* \xleftarrow{} 55.6\,^\circ\text{C isotropic}\ .$$

Dielectric measurements were made on two samples. The first set of measurements were carried out on an 18-μm-thick sample with a homeotropic molecular orientation, as shown in Fig. 2(a), achieved by coating the glass plates of the cell with the surfactant Quilon C. In the A^* phase, the measuring electric field is then parallel to the director, thus permitting direct measurement of $\varepsilon_{\parallel}$. By cooling down to the C^* phase, the measuring electric field makes an angle with the director and the measured dielectric permittivity is a mixture of contributions from ε_1 and ε_3, which we shall denote ε_{hom}. These measurements were made in the frequency range 10^2–10^6 Hz. The second set of measurements were carried out on a 50-μm-thick sample without any surface treatment except a cleaning with acetone, and a planar orientation [Fig. 2(b)] was achieved by slowly cooling from the isotropic to the smectic-A^* phase in the presence of an ac electric field. In this geometry, the measuring electric field is applied parallel to the smectic layers and perpendicular to the director in the A^* phase, thus yielding $\varepsilon_\perp$. In the C^* phase, the measurements were first made in the presence of the helix and at 100 kHz to exclude the contribution of the Goldstone mode. We will denote the

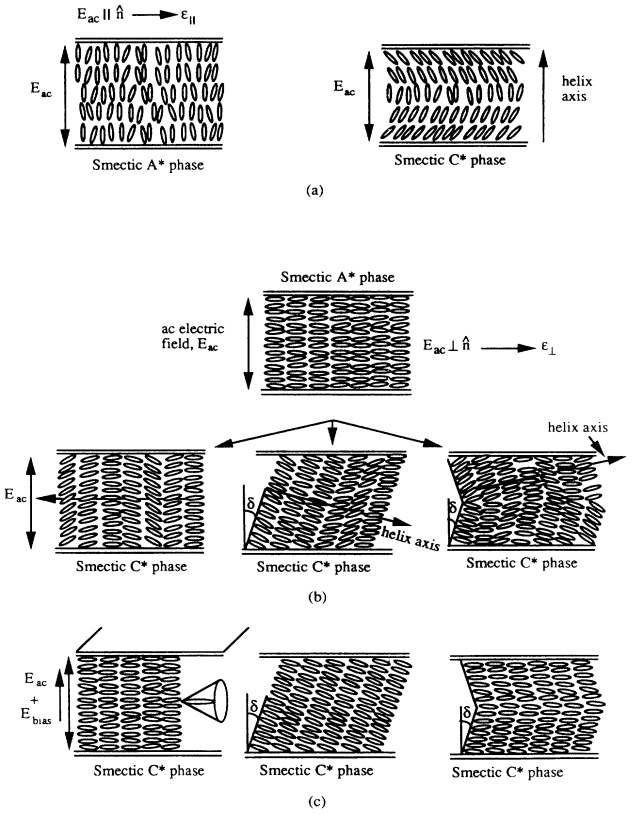

FIG. 2. Different measurement geometries in the smectic-A^* and C^* phases. (a) In the A^* phase, the smectic layers are aligned parallel to the glass plates. This geometry permits direct measurements of $\varepsilon_{\parallel}$. In the C^* phase, the smectic layers are still parallel to the glass plates, however, the director makes a tilt angle θ with E_{ac}. The measured dielectric permittivity in this case is denoted ε_{hom}. (b) In the A^* phase, the smectic layers are aligned perpendicular to the glass plates, i.e., upright bookshelf geometry. This measurement geometry permits direct measurement of $\varepsilon_\perp$. By cooling down to the C^* phase, the helical structure appears and one may get an upright bookshelf geometry, or homogeneously tilted smectic layers, or chevron structure. The measured dielectric permittivity of all three geometries is denoted $\varepsilon_{\text{helix}}$. (c) By applying a bias electric field E_{bias} in a direction parallel to E_{ac}, the helix disappears and we get a new measurement geometry called the unwound state. In this case the measured dielectric permittivity is denoted ε_{unw}.

measured dielectric permittivity in this case by ε_{helix}. In the same cell, with the same measuring geometry, a bias electric field is then applied to unwind the helix [Fig. 2(c)]. The bias field was varied between 0 and ±35 V/50 μm. The measured value of dielectric permittivity in this case is denoted ε_{unw}. The temperature dependence of $\varepsilon_\perp$ and $\varepsilon_\parallel$ in the A^* phase, and ε_{helix}, ε_{unw}, and ε_{hom} in the C^* phase at low frequency, is shown in Fig. 3(a). In Fig. 3(b), we show the same measurements at low and high frequencies. Low- and high-frequency values of $\varepsilon_\parallel$ in the A^* phase and ε_{hom} in the C^* phase were extracted from Cole-Cole plots. The bias field dependence of the measured dielectric permittivity in the planar orientation is shown in Fig. 4.

III. THEORY

The aim of this section is to show how the three principal values of ε_1, ε_2, and ε_3 of the dielectric tensor, i.e., the intrinsic material parameters, can be extracted from the three measured cell permittivities that are not (at least not *a priori)* molecular properties but involve different contributions of tensor components depending on geometry.

Before proceeding, we show in Fig. 5 the relative orientation of the local tensor ellipsoid and our basic reference frame containing two of the axes along which the electric

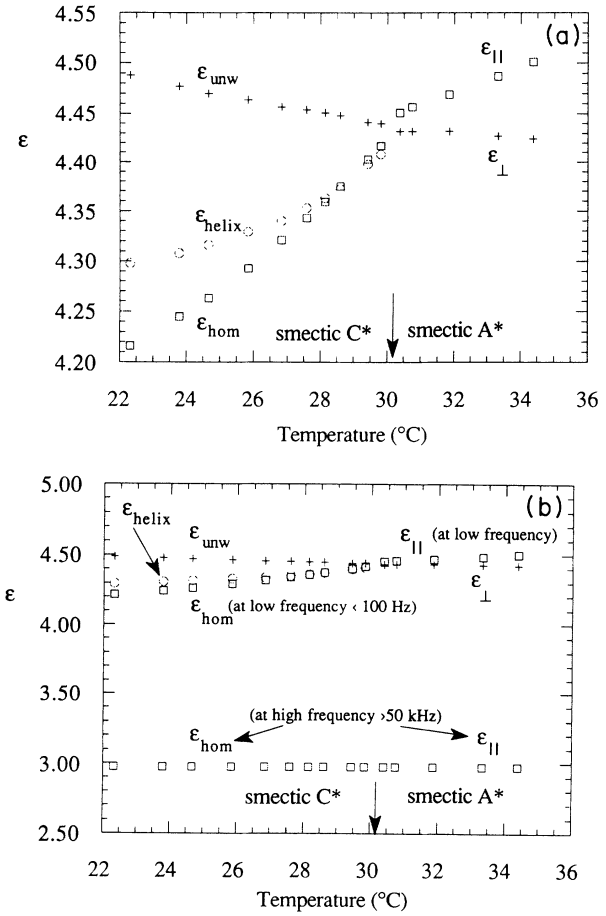

FIG. 3. (a) Temperature dependence of the measured dielectric permittivity at *low* frequency in the planar orientation (ε_{helix},ε_{unw}) in the C^* phase, ($\varepsilon_\perp$) in the A^* phase; in the homeotropic orientation (ε_{hom}) in the C^* phase, ($\varepsilon_\parallel$) in the A^* phase. (b) Temperature dependence of the dielectric permittivity measured at *high* frequency in the planar orientation (ε_{helix},ε_{unw}) in the C^* phase, ($\varepsilon_\perp$) in the A^* phase; in the homeotropic orientation (ε_{hom}, shown at low and high frequencies) in the C^* phase ($\varepsilon_\parallel$, shown at low and high frequencies) and in the A^* phase.

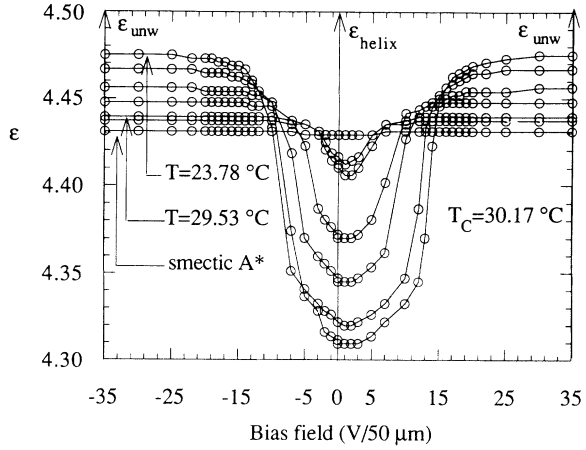

FIG. 4. Bias-electric-field dependence of the dielectic permittivity measured in the planar orientation at different temperatures in the C^* phase, and at one temperature in the A^* phase.

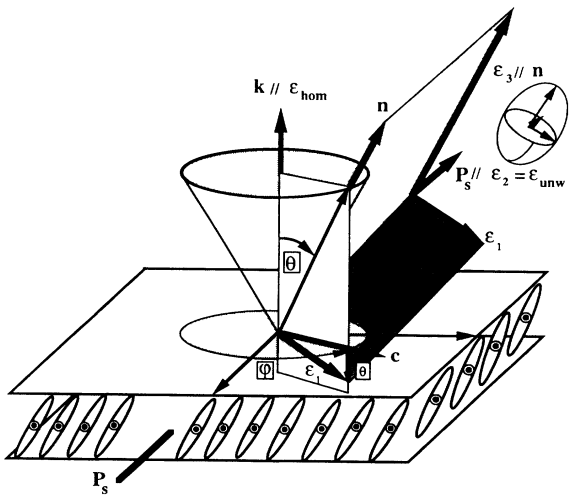

FIG. 5. Relative orientation of the dielectric tensor components ε_1, ε_2, and ε_3 with respect to the measured dielectric permittivity ε_{hom} and ε_{unw}. The director **n** is tilted with respect to the layer normal **k** with a tilt angle θ. The tilt direction is denoted by a unit vector **c** lying in the plane of the layer, which in the case of a chiral smectic-*C* phase, processes from layer to layer resulting in a helical structure with a helical axis in the direction of **k**. The chiral smectic-*C* phase has a local spontaneous polarization P_S in a direction parallel to (**k**×**n**), lying in the smectic plane. The component ε_1 lies in the tilt plane and ε_2 and ε_3 are parallel to the spontaneous polarization P_S and the director **n**, respectively.

measuring field is applied. Except for the layer inclination δ relative to the cell-plate normal, relevant variables used in the calculations are also defined in this figure.

Let us take the local frame as (x_1,x_2,x_3) coinciding with the local ellipsoid $(\varepsilon_1,\varepsilon_2,\varepsilon_3)$, and give new designation to the lab frame following successive coordinate transformations. Taking into consideration the molecular tilt θ, the tilt direction φ, and the smectic layer tilt δ, it is obvious that one has to carry out three successive tensor transformations of the Cartesian coordinates attached to the local ellipsoid of dielectric permittivity in the following way.

(i) Rotation of the Cartesian coordinates (x_1,x_2,x_3) through an angle θ around the x_2 axis. This leads to $(x_1,x_2,x_3)\rightarrow(x_1',x_2',x_3')$. The ε tensor, in the new frame, is denoted $\varepsilon(\theta)$.

(ii) Rotation of the Cartesian coordinates (x_1',x_2',x_3') through an angle φ around the x_3' axis, leading to $(x_1',x_2',x_3')\rightarrow(x_1'',x_2'',x_3'')$. The ε tensor, in the new laboratory frame, is denoted $\varepsilon(\theta,\varphi)$.

(iii) Rotation of the Cartesian coordinates (x_1'',x_2'',x_3'') through an angle δ around the x_1'' axis, leading to $(x_1'',x_2'',x_3'')\rightarrow(x_1''',x_2''',x_3''')$. The ε tensor, in the new laboratory frame, is denoted $\varepsilon(\theta,\delta,\varphi)$.

The tensor $\varepsilon(\theta)$ is obtained by the following transformation:

$$\varepsilon(\theta)=T_\theta\varepsilon T_\theta^T\ , \tag{1}$$

where ε and T_θ are given by

$$\varepsilon=\begin{bmatrix}\varepsilon_1 & 0 & 0\\ 0 & \varepsilon_2 & 0\\ 0 & 0 & \varepsilon_3\end{bmatrix}\ , \tag{2a}$$

$$T_\theta=\begin{bmatrix}\cos\theta & 0 & \sin\theta\\ 0 & 1 & 0\\ -\sin\theta & 0 & \cos\theta\end{bmatrix}\ , \tag{2b}$$

and T_θ^T is the transpose of T_θ. The explicit form of $\varepsilon(\theta)$ may be written as

$$\varepsilon(\theta)=\begin{bmatrix}\varepsilon_1\cos^2\theta+\varepsilon_3\sin^2\theta & 0 & (\varepsilon_3-\varepsilon_1)\sin\theta\cos\theta\\ 0 & \varepsilon_2 & 0\\ (\varepsilon_3-\varepsilon_1)\sin\theta\cos\theta & 0 & \varepsilon_1\sin^2\theta+\varepsilon_3\cos^2\theta\end{bmatrix}\ , \tag{3a}$$

$$\varepsilon(\theta)=\begin{bmatrix}\varepsilon_\perp' & 0 & \Delta\varepsilon\sin\theta\cos\theta\\ 0 & \varepsilon_2 & 0\\ \Delta\varepsilon\sin\theta\cos\theta & 0 & \varepsilon_\parallel'\end{bmatrix}\ , \tag{3b}$$

where

$$\varepsilon_\perp'=\varepsilon_1\cos^2\theta+\varepsilon_3\sin^2\theta\ ,$$

$$\varepsilon_\parallel'=\varepsilon_1\sin^2\theta+\varepsilon_3\cos^2\theta\ ,$$

and

$$\Delta\varepsilon=\varepsilon_3-\varepsilon_1\ .$$

The tensor $\varepsilon(\theta,\varphi)$ is given by

$$\varepsilon(\theta,\varphi)=T_\varphi\varepsilon(\theta)T_\varphi^T\ , \tag{4}$$

with T_φ, in this case, being

$$T_\varphi=\begin{bmatrix}\cos\varphi & -\sin\varphi & 0\\ \sin\varphi & \cos\varphi & 0\\ 0 & 0 & 1\end{bmatrix}\ . \tag{5}$$

After performing the transformation, $\varepsilon(\theta,\varphi)$ is found to be

$$\varepsilon(\theta,\varphi)=\begin{bmatrix}\varepsilon_\perp'\cos^2\varphi+\varepsilon_2\sin^2\varphi & (\varepsilon_\perp'-\varepsilon_2)\sin\varphi\cos\varphi & \Delta\varepsilon\sin\theta\cos\theta\cos\varphi\\ (\varepsilon_\perp'-\varepsilon_2)\sin\varphi\cos\varphi & \varepsilon_\perp'\sin^2\varphi+\varepsilon_2\cos^2\varphi & \Delta\varepsilon\sin\theta\cos\theta\sin\varphi\\ \Delta\varepsilon\sin\theta\cos\theta\cos\varphi & \Delta\varepsilon\sin\theta\cos\theta\sin\varphi & \varepsilon_\parallel'\end{bmatrix}\ . \tag{6}$$

In thick cells, one has to average over the angle φ for a length corresponding to the helical pitch. This gives

$$\langle\varepsilon(\theta,\varphi)\rangle_\varphi=\begin{bmatrix}\frac{1}{2}(\varepsilon_1\cos^2\theta+\varepsilon_3\sin^2\theta+\varepsilon_2) & 0 & 0\\ 0 & \frac{1}{2}(\varepsilon_1\cos^2\theta+\varepsilon_3\sin^2\theta+\varepsilon_2) & 0\\ 0 & 0 & \varepsilon_1\sin^2\theta+\varepsilon_3\cos^2\theta\end{bmatrix}\ . \tag{7a}$$

The tensor $\langle\varepsilon(\theta,\varphi)\rangle_\varphi$ is diagonal in the laboratory frame x_1'',x_2'',x_3''. Its describes a *uniaxial* crystal with the symmetry axis parallel to the x_3'' axis, i.e., the helix axis. Thus it makes sense to rewrite the tensor to clarify the uniaxiality in the form

$$\langle\varepsilon\rangle=\begin{bmatrix}\langle\varepsilon_\perp\rangle & 0 & 0\\ 0 & \langle\varepsilon_\perp\rangle & 0\\ 0 & 0 & \langle\varepsilon_\parallel\rangle\end{bmatrix}\ , \tag{7b}$$

where

$$\langle \varepsilon_\perp \rangle = \tfrac{1}{2}(\varepsilon_1 \cos^2\theta + \varepsilon_3 \sin^2\theta + \varepsilon_2) ,$$

$$\langle \varepsilon_\parallel \rangle = \varepsilon_1 \sin^2\theta + \varepsilon_3 \cos^2\theta .$$

Finally, the tensor $\varepsilon(\theta,\delta,\varphi)$ [or $\langle \varepsilon(\delta) \rangle$] can be written as

$$\langle \varepsilon(\delta) \rangle = T_\delta \langle \varepsilon \rangle T_\delta^T , \tag{8}$$

where T_δ is the matrix

$$T_\delta = \begin{bmatrix} 1 & 1 & 0 \\ 0 & \cos\delta & -\sin\delta \\ 0 & \sin\delta & \cos\delta \end{bmatrix} \tag{9}$$

and the tensor $\langle \varepsilon(\delta) \rangle$ is given by

$$\langle \varepsilon(\delta) \rangle = \begin{bmatrix} \langle \varepsilon_\perp \rangle & 0 & 0 \\ 0 & \langle \varepsilon_\perp \rangle \cos^2\delta + \langle \varepsilon_\parallel \rangle \sin^2\delta & (\langle \varepsilon_\perp \rangle - \langle \varepsilon_\parallel \rangle) \sin\delta \cos\delta \\ 0 & (\langle \varepsilon_\perp \rangle - \langle \varepsilon_\parallel \rangle) \sin\delta \cos\delta & \langle \varepsilon_\perp \rangle \sin^2\delta + \langle \varepsilon_\parallel \rangle \cos^2\delta \end{bmatrix} \begin{matrix} \\ \\ \langle \varepsilon_\perp \rangle \cos\delta \longrightarrow \langle \varepsilon_1 \rangle \cos^2\delta \end{matrix} . \tag{10}$$

When measuring on samples having planar orientation, the measuring electric field in the laboratory frame is applied in the x_2''' direction. As we also measure the response in this direction, the relevant dielectric value is given by the ε_{22} element of the $\langle \varepsilon(\delta) \rangle$ matrix. The measured value is denoted $\varepsilon_{\text{helix}}$. It follows from (10) that it is given by

$$\begin{aligned} \varepsilon_{\text{helix}} &= \langle \varepsilon_\perp \rangle \cos^2\delta + \langle \varepsilon_\parallel \rangle \sin^2\delta \\ &= \tfrac{1}{2}(\varepsilon_1 \cos^2\theta + \varepsilon_3 \sin^2\theta + \varepsilon_2)\cos^2\delta \\ &\quad + (\varepsilon_1 \sin^2\theta + \varepsilon_3 \cos^2\theta)\sin^2\delta . \end{aligned} \tag{11}$$

In the homeotropic orientation, the measuring electric field is applied in the x_3''' direction. The measured value is denoted ε_{hom}, and is equal to

$$\begin{aligned} \varepsilon_{\text{hom}} &= \langle \varepsilon_\perp \rangle \sin^2\delta + \langle \varepsilon_\parallel \rangle \cos^2\delta \\ &= \tfrac{1}{2}(\varepsilon_1 \cos^2\theta + \varepsilon_3 \sin^2\theta + \varepsilon_2)\sin^2\delta \\ &\quad + (\varepsilon_1 \sin^2\theta + \varepsilon_3 \cos^2\theta)\cos^2\delta . \end{aligned} \tag{12}$$

Equation (12) is applicable if, in the homeotropic orientation, the smectic layers are tilted. However, in practice, *unless* the sample is cooled down in the presence of an external field, the director is tilted and the smectic layers are kept fixed parallel to the glass plates. This is verified by conoscopic observations. Therefore, the proper expression for ε_{hom} in our case is rather the element ε_{33} in the $\langle \varepsilon(\theta,\varphi) \rangle_\varphi$ tensor, thus

$$\varepsilon_{\text{hom}} = \varepsilon_1 \sin^2\theta + \varepsilon_3 \cos^2\theta . \tag{13}$$

To get an expression for the dielectric permittivity ε_{unw} measured in the planar orientation in the presence of a bias electric field (helix-free samples), the tensor $\varepsilon(\theta)$ according to Eq. (3) is rotated by an angle δ resulting in the tensor $\varepsilon(\theta,\delta)$ using the transformation matrix T_δ,

$$\varepsilon(\theta,\delta) = T_\delta \varepsilon(\theta) T_\delta^T . \tag{14}$$

The tensor $\varepsilon(\theta,\delta)$ is then found to be

$$\varepsilon(\theta,\delta) = \begin{bmatrix} \varepsilon_1 \cos^2\theta + \varepsilon_3 \sin^2\theta & -\Delta\varepsilon \sin\theta \cos\theta \sin\delta & \Delta\varepsilon \sin\theta \cos\theta \cos\delta \\ -\Delta\varepsilon \sin\theta \cos\theta \sin\delta & \varepsilon_2 \cos^2\delta + \langle \varepsilon_\parallel \rangle \sin^2\delta & -(\varepsilon_2 - \langle \varepsilon_\parallel \rangle)\sin\delta \cos\delta \\ \Delta\varepsilon \sin\theta \cos\theta \cos\delta & -(\varepsilon_2 - \langle \varepsilon_\parallel \rangle)\sin\delta \cos\delta & \varepsilon_2 \sin^2\delta + \langle \varepsilon_\parallel \rangle \cos^2\delta \end{bmatrix} . \tag{15}$$

In a planar sample, in the presence of both measuring and bias electric fields, the measured permittivity ε_{unw} is then given by

$$\begin{aligned} \varepsilon_{\text{unw}} &= \varepsilon_2 \cos^2\delta + \langle \varepsilon_\parallel \rangle \sin^2\delta \\ &= \varepsilon_2 \cos^2\delta + (\varepsilon_1 \sin^2\theta + \varepsilon_3 \cos^2\theta)\sin^2\delta . \end{aligned} \tag{16}$$

In a homeotropic sample, in the case of a helix-free cell with tilted smectic layers, ε_{hom} is given by

$$\begin{aligned} \varepsilon_{\text{hom}} &= \varepsilon_2 \sin^2\delta + \langle \varepsilon_\parallel \rangle \cos^2\delta \\ &= \varepsilon_2 \sin^2\delta + (\varepsilon_1 \sin^2\theta + \varepsilon_3 \cos^2\theta)\cos^2\delta . \end{aligned} \tag{17}$$

Equations (11) and (16) relate the three components ε_1, ε_2, and ε_3 of the ε tensor to the measured dielectric permittivities $\varepsilon_{\text{helix}}$ and ε_{unw} in the planar orientation, taking into consideration the smectic layer tilt. Equation (13) connects the components ε_1 and ε_3 to the measured dielectric permittivity ε_{hom} in the case of homeotropic orientation as discussed previously. If the smectic layers are standing perpendicular to the glass plates, the corresponding set of equations can be obtained by letting δ go to zero,

$$\varepsilon_{\text{helix}} = \tfrac{1}{2}(\varepsilon_1 \cos^2\theta + \varepsilon_3 \sin^2\theta + \varepsilon_2) , \tag{18a}$$

$$\varepsilon_{\text{unw}} = \varepsilon_2 . \tag{18b}$$

Equations (13), (18a), and (18b) are the same as those obtained by Hoffman *et al.*

In order to evaluate the molecular permittivities ε_1, ε_2, and ε_3, Eqs. (11), (13), and (16) can be rewritten as

$$\varepsilon_1=\frac{1}{1-2\sin^2\theta}\left[\frac{\cos^2\theta}{\cos^2\delta}(2\varepsilon_{\text{helix}}-\varepsilon_{\text{unw}}-\varepsilon_{\text{hom}}\sin^2\delta)-\varepsilon_{\text{hom}}\sin^2\theta\right], \quad (19)$$

$$\varepsilon_2=\frac{1}{\cos^2\delta}(\varepsilon_{\text{unw}}-\varepsilon_{\text{hom}}\sin^2\delta), \quad (20)$$

$$\varepsilon_3=\frac{-1}{1-2\sin^2\theta}\left[\frac{\sin^2\theta}{\cos^2\delta}(2\varepsilon_{\text{helix}}-\varepsilon_{\text{unw}}-\varepsilon_{\text{hom}}\sin^2\delta)-\varepsilon_{\text{hom}}\cos^2\theta\right]. \quad (21)$$

Values of ε_1, ε_2, and ε_3 have also been calculated when δ is assumed equal to zero in the case of planar and homeotropic orientations using the following formulas:

$$\varepsilon_1=\frac{1}{1-2\sin^2\theta}[\cos^2\theta(2\varepsilon_{\text{helix}}-\varepsilon_{\text{unw}})-\varepsilon_{\text{hom}}\sin^2\theta], \quad (22)$$

$$\varepsilon_2=\varepsilon_{\text{unw}}, \quad (23)$$

$$\varepsilon_3=\frac{-1}{1-2\sin^2\theta}[\sin^2\theta(2\varepsilon_{\text{helix}}-\varepsilon_{\text{unw}})-\varepsilon_{\text{hom}}\cos^2\theta]. \quad (24)$$

IV. RESULTS AND DISCUSSION

It is obvious from Eqs. (19)–(24) that in order to calculate the values ε_1, ε_2, and ε_3, the tilt angle θ has to be determined at different temperatures in the C^* phase. In the present work, we have determined the tilt angle (see Fig. 6) using a method that we have described elsewhere [9] and that enables us to use the already performed dielectric measurements carried out in homeotropic orientation.

In addition to the knowledge of θ, the evaluation of correct values of ε_1, ε_2, and ε_3 requires, in principle, knowledge of the layer tilt, which cannot be inferred from any of our measurements. As shown by the x-ray studies performed by Rieker *et al.* [6], δ increases below the $A\rightarrow C$ transition point in a way that is similar to the increase in the tilt angle θ, being generally somewhat smaller than θ. Often $\delta=0.8\theta$ is taken as an approximate value. Our evaluation of dielectric constants is not affected by choosing 0.8θ rather than θ, and in fact, values $\delta\neq 0$ happen to have only a minor effect on the obtained ε values. The temperature dependence of the determined values of ε_1, ε_2, and ε_3 at low and high frequencies are shown in Figs. 7(a) and 7(b), respectively.

In order to discuss the validity of the measuring method and the methodologic error introduced by our simplified models, we may go back to Fig. 2. In the three drawings representing quasibookshelf geometry with helix [Fig. 2(b)], no attempt has been made to illustrate the surface actions from the glass plates (trying to force the molecules to be parallel to the surfaces), as bulk properties are dominating the thick samples anyway. Moreover, the details for the bulk organization of the mole-

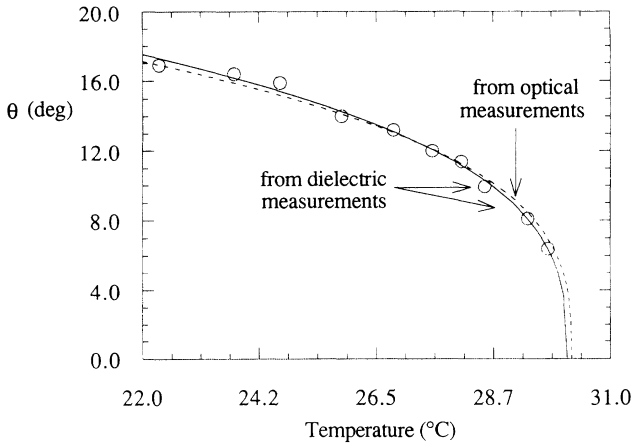

FIG. 6. Temperature dependence of the determined tilt angle using dielectric measurements (circles), compared with the optically measured tilt angle (dotted line).

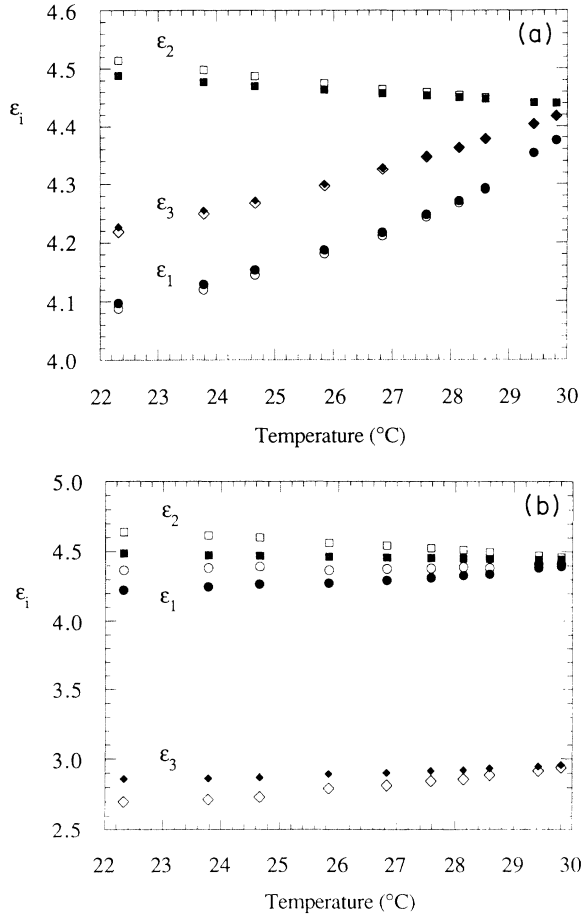

FIG. 7. (a) Temperature dependence of the three components of the dielectric tensor at *low* frequency in the C^* phase. Solid and open symbols represent results obtained assuming bookshelf geometry and tilted smectic layers, respectively. (b) Temperature dependence of the three components of the dielectric tensor at *high* frequency in the C^* phase. Solid and open symbols represent results obtained assuming upright bookshelf geometry and tilted smectic layers, respectively.

cules in the case of the helix being present is not known. For instance, if we have a chevron structure, the chevron interface will act as a third surface with a rather powerful torque on the molecules, turning them into the same horizontal direction as the glass plates. With the simplified model of evaluation, as depicted in Fig. 2(a), it is clear that we will overestimate the effect of layer tilt δ. The same is true for the geometry with unwound helix. Furthermore, by putting $\delta=\theta$ as discussed above, we make a choice that is in itself an overestimation of δ. A reasonable estimation of the maximum error due to the uncertainty or neglect of layer tilt can therefore be taken as the difference between the evaluated values for $\delta\neq 0$ [Eqs. (19)–(21)] and those evaluated as if δ were zero [Eqs. (22)–(24)]. As an illustration, we have calculated the normalized values for ε_1, ε_2, and ε_3 with the corresponding $\varepsilon_i(\delta=0)$ as a normalizing factor. The relative error, in percent, has been plotted in Fig. 8(a). For this plot, the tilt angle θ has been kept fixed at 22.5° (even if the maximum measured value of our substance is about 16°), and the values of $\varepsilon_{\text{helix}}$, ε_{unw}, and ε_{hom} have been chosen to be 4.5, 5.0, and 3.0, respectively. As we see, the errors in ε_1 and ε_2 are less than 7% or 6% and in ε_3 less than 2%. In Fig. 8(b), the corresponding errors in $\Delta\varepsilon$ and $\delta\varepsilon$ are shown. As can be seen, our evaluation method tends to overestimate $\Delta\varepsilon$ and $\delta\varepsilon$, but the errors are well within 10% and in most of the interval are quite smaller. Another source of error comes from the fact that ε_1, ε_2, and ε_3 are evaluated as differences of quantities that not only are inexact in themselves but may have (ε_{hom}) an error that depends on frequency. This may simulate (a very slight) unphysical frequency dependence in ε_1 and ε_2; cf. Figs. 7(a) and 7(b). However, the introduced error is at most the same order as the error connected with δ discussed above.

The symmetry properties of the dielectric anisotropy $\Delta\varepsilon$ and the dielectric biaxiality $\delta\varepsilon$ are quite different. At the tilting transition, i.e., at loss of cylindrical symmetry, $\Delta\varepsilon$ reflects mainly the change of ε_1, as ε_3 can be considered constant to first order in θ. Thus for small tilt, $\Delta\varepsilon$ can be expected to grow linearly with θ. The splitting up of $\varepsilon_\perp$ in the two values of ε_1 and ε_2, i.e., the biaxiality, ought to be independent of the sign of the tilt, hence $\delta\varepsilon$ should be quadratic in the tilt angle θ. As for this angle, the temperature dependence has been fitted to a power

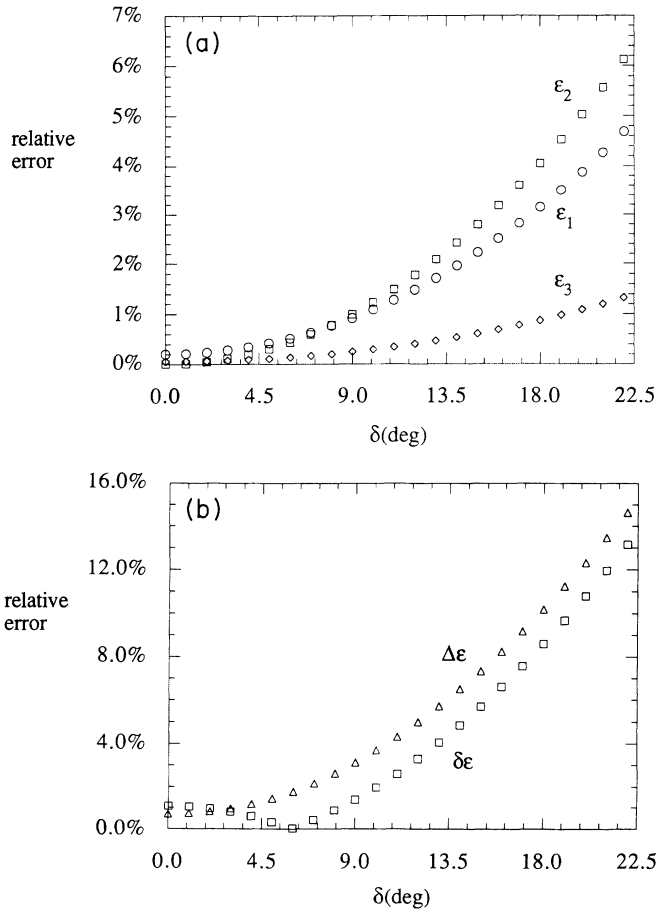

FIG. 8. (a) Dependence of the relative error of ε_1, ε_2, and ε_3 on the smectic layer tilt angle δ. (b) Dependence of the relative error of $\Delta\varepsilon$ and $\delta\varepsilon$ on the smectic layer tilt angle δ.

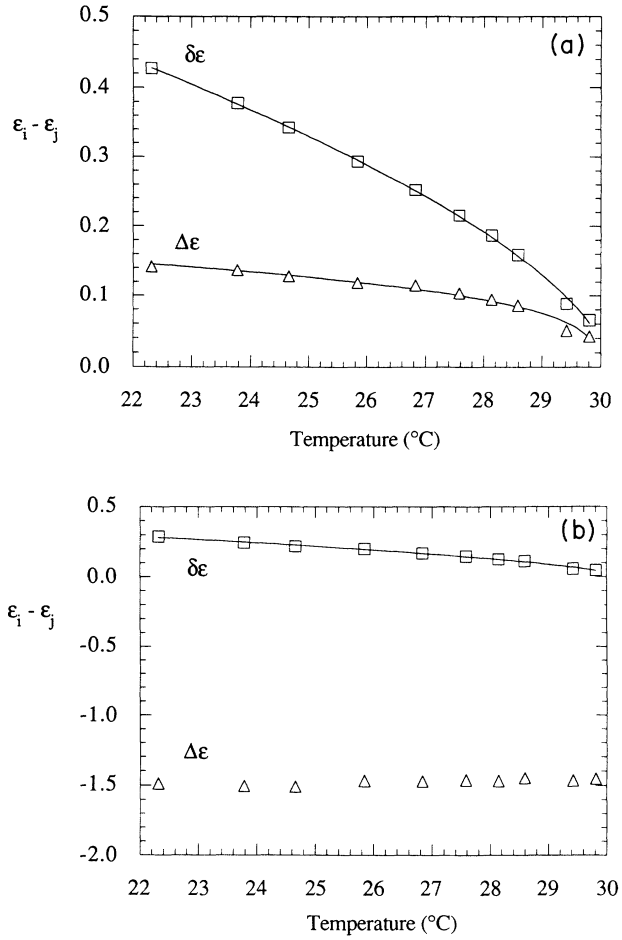

FIG. 9. (a) Temperature dependence of the dielectric anisotropy $\Delta\varepsilon$ and dielectric biaxiality $\delta\varepsilon$ in the C^* phase at how frequency. The subscript $i=2$ and 3, and $j=1$. (b) Temperature dependence of the dielectric anisotropy $\Delta\varepsilon$ and dielectric biaxiality $\delta\varepsilon$ in the C^* phase at high frequency. The subscript $i=2$ and 3, and $j=1$.

law

$$\theta = A\left[1-\frac{T}{T_C}\right]^{\beta} . \tag{25}$$

The critical exponent β is found to be approximately 0.30 (0.32 and 0.31, respectively). The temperature dependence of dielectric anisotropy and dielectric biaxiality is shown in Figs. 9(a) and 9(b) for low ($\approx$100 Hz) and high ($\approx$100 kHz) frequencies. The values have been fitted to the same power law as in Eq. (25). For the anisotropy $\Delta\varepsilon$ we expect, from the argument above, the critical exponent to be the same as for the tilt angle

$$\beta(\Delta\varepsilon)=\beta(\theta)\approx 0.30 ,$$

whereas for $\delta\varepsilon$ we should expect

$$\delta\varepsilon \propto \theta^2 \propto \left[1-\frac{T}{T_C}\right]^{2\beta} ,$$

thus

$$\beta(\delta\varepsilon)=2\beta(\theta)\approx 0.60 .$$

These expectations are reasonably well borne out by the experimental data.

The values of ε_1, ε_2, and ε_3 will be interesting in due time, when a sufficient body of empirical material has been collected to correlate with molecular structure, but they are also important for the electro-optic response and behavior of ferroelectric liquid crystals. In order to stabilize the molecular axis in high-contrast planar directions, materials would be preferable with $\delta\varepsilon=\varepsilon_2-\varepsilon_1>0$ together with $\varepsilon_3-\varepsilon_1<0$. These inequalities should be valid at frequencies corresponding to addressing pulse frequencies typical for FLC displays, that is, in the region 10–100 kHz. As can be seen, in our case $\delta\varepsilon$ is always positive, whereas $\varepsilon_3-\varepsilon_1$ is positive at low frequencies but negative at high frequencies, i.e., in the region of interest.

To conclude, we have calculated the three main components of the dielectric tensor in the C^* phase. It is found that the inequality

$$\varepsilon_2>\varepsilon_3>\varepsilon_1$$

holds at low frequency. However, at high frequency the inequality

$$\varepsilon_2>\varepsilon_1>\varepsilon_3$$

holds. This frequency dependence is attributed to the relaxation behavior of ε_3 assigned to the molecular rotation around the short molecular axis. At low frequency, the dielectric anisotropy is positive and its magnitude is less than the dielectric biaxiality $\delta\varepsilon$. However, at high frequency, $\Delta\varepsilon$ is negative and its magnitude is greater than $\delta\varepsilon$. If we go to very high, i.e., optical, frequencies it is well known [10] that even the smectic-C phase can, to a very good approximation, be considered to be uniaxial, which means that $\delta\varepsilon$ is negligible. As our measurements show, the biaxiality $\delta\varepsilon$ is on the contrary quite pronounced in the whole frequency region of importance for the electro-optic response.

[1] D. S. Parmar and Ph. Martinot-Lagarde, Ann. Phys. (Paris) **3**, 275 (1978).
[2] T. Geelhaar, Ferroelectrics **85**, 717 (1988).
[3] P. G. de Gennes, *The Physics of Liquid Crystals* (Oxford University Press, New York, 1974), p. 31.
[4] J. C. Jones, E. P. Raynes, and M. J. Towler, Mol. Cryst. Liq. Cryst. Lett. **7**, 91 (1990).
[5] J. Hoffmann, W. Kuczynski, J. Malecki, and J. Pavel, Ferroelectrics **76**, 61 (1987).
[6] T. P. Rieker, N. A. Clark, G. S. Smith, D. S. Parmar, E. B. Sirota, and C. R. Safinya, Phys. Rev. Lett. **59**, 2658 (1987).
[7] Y. Sato, T. Tanaka, M. Nagata, H. Takeshita, and S. Morozumi, Proc. SID **28**, 2189 (1987).
[8] J. C. Jones, E. P. Raynes, M. J. Towler, and J. R. Sambles, Mol. Cryst. Liq. Cryst. (to be published).
[9] F. Gouda, K. Skarp, S. T. Lagerwall, C. Escher, and H. Kresse, J. Phys. (Paris) I **1**, 167 (1991).
[10] S. Garoff, Ph.D. thesis, Harvard University, 1977.

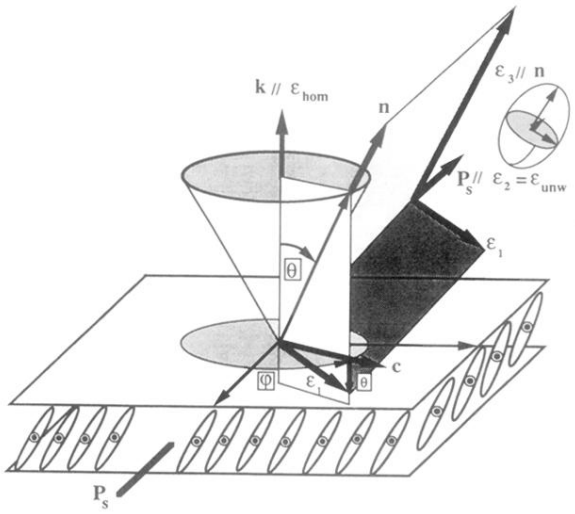

FIG. 5. Relative orientation of the dielectric tensor components ε_1, ε_2, and ε_3 with respect to the measured dielectric permittivity ε_{hom} and ε_{unw}. The director **n** is tilted with respect to the layer normal **k** with a tilt angle θ. The tilt direction is denoted by a unit vector **c** lying in the plane of the layer, which in the case of a chiral smectic-*C* phase, processes from layer to layer resulting in a helical structure with a helical axis in the direction of **k**. The chiral smectic-*C* phase has a local spontaneous polarization P_S in a direction parallel to $(\mathbf{k}\times\mathbf{n})$, lying in the smectic plane. The component ε_1 lies in the tilt plane and ε_2 and ε_3 are parallel to the spontaneous polarization P_S and the director **n**, respectively.